

MOL # 26989

**Monitoring the activation state of Insulin/IGF-1 hybrid receptors  
using Bioluminescence Resonance Energy Transfer**

**Christophe Blanquart, Carmen Gonzalez-Yanes and Tarik Issad**

**Institut Cochin**, Département de Biologie Cellulaire, Paris, F-75014 France.

**Inserm**, U567, Paris, F-75014 France.

**CNRS**, UMR 8104, Paris, F-75014 France.

**Université Paris Descartes**, Faculté de Médecine René Descartes, UM 3, Paris, F-75014  
France.

MOL # 26989

**Running title:** Specific study of IRA/IGF1R hybrids by BRET

**Corresponding author:**

**Dr. Tarik ISSAD**

Institut Cochin, Department of Cell Biology

22 Rue Méchain, 75014 PARIS - FRANCE

**Tel: (331)-40-51-64-09; Fax: (331)-40-51-64-30; email: [issad@cochin.inserm.fr](mailto:issad@cochin.inserm.fr)**

**32 text pages**

**9 figures**

**0 table**

**35 references**

**Abstract: 244 words**

**Introduction: 745 words**

**Discussion: 846 words**

Abbreviations:

**IGF1R, Insulin-like Growth Factor-1 Receptor; IRA, Insulin Receptor isoform A; Rluc, *Renilla* luciferase; WT, Wild Type; KD, Kinase Dead; TK, Tyrosine Kinase; YFP, Yellow Fluorescent Protein; WGL, Wheat-Germ Lectin; SDS-PAGE, sodium dodecyl sulfate polyacrylamide gel electrophoresis; PTP1B, Protein Tyrosine Phosphatase 1B; BRET, Bioluminescence Resonance Energy Transfer; mBU, milliBRET Unit; DMEM, Dulbecco's Modified Eagle's Medium.**

MOL # 26989

## Abstract

In cells expressing both the insulin receptor isoform A (IRA) and the insulin like growth factor-1 receptor (IGF1R), the presence of hybrid receptors, constituted of an  $\alpha\beta$ -IRA chain associated with an  $\alpha\beta$ -IGF1R chain, has been demonstrated. These heterodimers are found in normal cells, and also appear to play crucial roles in a number of cancers. However, they remain difficult to study, due to the concomitant presence of IRA and IGF1R homodimers. Using bioluminescence resonance energy transfer (BRET), we have developed assays to specifically monitor the activation state of IRA/IGF1R hybrids, both *in vitro* and in living cells. The first assay allowed the study of ligand-induced conformational changes within hybrid receptors purified from cells co-transfected with one type of receptor fused to *Renilla* luciferase (Rluc) and the other type of receptor fused to yellow fluorescent protein (YFP). In these conditions, only hybrid receptors were BRET competent. In the second assay, the activation state of IRA/IGF1R hybrids was monitored in real time, in living cells, by co-transfection of kinase-dead versions of IRA-Rluc or IGF1R-Rluc, wild-type untagged IRA or IGF1R, and a YFP-tagged soluble version of the substrate-trapping mutant of protein tyrosine-phosphatase 1B (YFP-PTP1B-D181A-Cter). In hybrid receptors, trans-phosphorylation of the kinase-dead  $\alpha\beta$ -Rluc moiety by the wild-type  $\alpha\beta$  moiety induced the recruitment of YFP-PTP1B-D181A-Cter, resulting in a hybrid-specific ligand-induced BRET signal. Therefore, both methods allow monitoring of the activity of IRA/IGF1R hybrid receptor and could be used to detect molecules of therapeutic interest for the treatment of cancer.

MOL # 26989

## Introduction

Insulin and IGF-1 exert their effects through tyrosine kinase (TK) receptors composed of two  $\alpha$ -chains that bind ligands and two  $\beta$ -chains that possess an intrinsic TK activity. These chains are held together by disulfide bonds. Binding of ligands induces trans-autophosphorylation of the  $\beta$ -chains on tyrosines, thereby stimulating the TK activity of these receptors toward intracellular substrates. The insulin receptor (IR) exists under two isoforms in cells (IRA or -exon 11 and IRB or + exon 11), as a result of alternative splicing of exon 11, which encodes the 12 carboxyl terminus amino-acids of the  $\alpha$ -chain (Moller et al., 1989). IRA and IRB display different pharmacological properties. Indeed, whereas insulin binds to IRA and IRB with high-affinity, insulin like growth factor-2 (IGF-2) binds to and activates IRA but not IRB (Frasca et al., 1999). Both isoforms can transmit metabolic signals, such as glucose transport and metabolism, and displays mitogenic and anti-apoptotic properties. However, IRA and IRB present different expression pattern. Indeed, IRA is expressed mainly in foetal tissues and adult brain and kidney (Frasca et al., 1999), whereas IRB is expressed predominantly in adult liver, muscle and adipose tissues, the main target tissues of insulin action (Moller et al., 1989; Mosthaf et al., 1990). Over-expression of IRA is observed in several tumors (Sciacca et al., 1999; Pandini et al., 1999), and IRA level has been correlated with the level of de-differentiation of thyroid cancer cells (Vella et al., 2002). Moreover, IRA has been implicated in a positive autocrine/paracrine loop, resulting in cell proliferation in IGF-2 producing tumors (Sciacca et al., 1999). All these observations confer to IRA a major function in cancer (Denley et al., 2003). IGF1R is a widely expressed receptor that shares strong homology with the IR. The IGF1R has been implicated in several physiological and pathophysiological processes. Physiologically, this receptor plays a major function in the transmission of growth promoting effects of IGF-1. In addition, IGF1R displays mitogenic, anti-apoptotic and transforming properties and has been involved in various types of cancers,

MOL # 26989

including prostate, thyroid and breast cancers (O'Connor, 2003; Pollak, 2004; Vella et al., 2001).

Several studies have demonstrated the existence of IRA/IGF1R hybrid receptors, constituted of heterodimers containing an  $\alpha\beta$  chain of the IR associated with an  $\alpha\beta$  chain of the IGF1R, both in normal (Soos et al., 1993; Soos and Siddle, 1989; Soos et al., 1990) and cancer cells (Pandini et al., 1999). Increased representation of these hybrids can be observed in several tumor cells as the result of an over-expression of IR and/or IGF1R (Pandini et al., 1999; Vella et al., 2001). The pharmacological properties of these hybrids appear to be different from those of their homodimers counterparts and depend on the IR isoform involved. The IRA/IGF1R hybrid receptors are strongly activated by IGF-1 and IGF-2 and weakly activated by insulin, whereas the IRB/IGF1R hybrid receptors are strongly activated by IGF-1, weakly activated by IGF-2 and poorly activated by insulin (Pandini et al., 2002). Although the biological role of IRA/IGF1R hybrids remains unclear, they appear to have a major function in tumors (Belfiore et al., 1999; Pandini et al., 1999). Therefore, the IRA/IGF1R hybrid receptor constitutes an important therapeutic target for the development of anti-cancer drugs. However, the study of these hybrids is rendered difficult by the presence of the homodimeric form of each receptor (IRA/IRA and IGF1R/IGF1R). In this work, we aimed to set-up procedures, based on BRET, that can be used to specifically study the activation state of the IRA/IGF1R hybrid receptors.

To study the interaction between two partners using BRET, one partner is fused to *Renilla* luciferase (Rluc) and the other to the yellow fluorescent protein (YFP) (Xu et al., 1999). The luciferase is excited by its substrate, coelenterazine. If the two partners are less than 100Å apart, an energy transfer occurs between the luciferase and the YFP, and a signal, emitted by the YFP, can be detected at 530 nm. We previously used this technology to monitor ligand-induced conformational changes within IR (Boute et al., 2001) and IGF1R (Blanquart et al., 2005). We also used BRET to study the dynamics of interaction of IR with PTP1B (Boute et

MOL # 26989

al., 2003), PTP $\alpha/\epsilon$  (Lacasa et al., 2005), and with Grb14 (Nouaille et al., 2006). We also showed that the interaction between IGF1R and PTP1B can be studied by BRET (Blanquart et al., 2005). In the present report, we have developed methods to specifically monitor the activation state of IRA/IGF1R hybrid receptors, both *in vitro* and in intact living cells.

MOL # 26989

## Materials and Methods

### Materials

All reagents have been described previously (Blanquart et al., 2005; Boute et al., 2003; Boute et al., 2001; Lacasa et al., 2005). Briefly, IGF1 and IGF2 were from Sigma-Aldrich Laborchemikalien (Seelze, Germany), human insulin was from Lilly France, (Suresnes, France), anti-IR $\beta$  and anti-IGF1 $\beta$  antibodies were from Santa Cruz Biotechnology (Santa Cruz, CA), 4G10 anti-phosphotyrosine antibody was from UBI (Lake Placid, NY, USA) and PTP1B monoclonal antibody was from Calbiochem (San Diego, CA, USA).

### Expression vectors

The cDNAs coding for the insulin receptor isoform A (IRA) in pcDNA3 used in this study (IRA, IRA-Rluc and IRA-YFP) were obtained by replacing the BstX-I fragment of their IRB counterparts (IRB, IRB-Rluc and IRB-YFP) by the BstX-I fragment of IRA in pECE vector (Ellis et al., 1986). The IGF1R-Rluc, IGF1R-YFP and YFP-PTP1B-D181A-Cter expression vectors have been described previously (Blanquart et al., 2005; Boute et al., 2003). pEYFP-C1 expression vector was from Clontech (Mountain View, CA, USA).

The cDNA coding for kinase-dead IGF1R mutants (IGF1R<sub>KD</sub>-Rluc and IGF1R<sub>KD</sub>-YFP) were obtained by directed mutagenesis of the lysine 1003 in alanine on, respectively, the IGF1R-Rluc and IGF1R-YFP expression vectors using the following oligonucleotides: Forward, 5' CCAGAGTGGCCATTGCAACAGTGAACGAGGCCG 3' and reverse, 5' CGGCCTCGTTCCTGTTGCAATGGCCAGTCTGG 3'. The IRA<sub>KD</sub>-Rluc cDNA was obtained by replacing the Ssp-I fragment of pcDNA3 IRB<sub>KD</sub>-Rluc (Nouaille et al., 2006) by the Ssp-I fragment of pcDNA3-IRA-Rluc. The cDNA coding for IRA<sub>KD</sub>-YFP was obtained by replacing the BstX-I fragment of pcDNA3 IRA-YFP vector by the BstX-I fragment of pcDNA3-IRA<sub>KD</sub>-Rluc vector.

MOL # 26989

### **Cell culture, transfection, and partial purification of tyrosine kinase fusion proteins.**

HEK-293 cells maintained in Dulbecco's Modified Eagles's Medium (DMEM, Invitrogen, Cergy Pontoise, France) supplemented with 4.5 g/l glucose and 10% fetal bovine serum were seeded at a density of  $2.5 \times 10^5$  cells per 35 mm dish. Transient transfections were performed 1 day later using FuGENE 6 (Roche Diagnostics, Indianapolis, IN, USA) according to the manufacturer's protocol. For partial purification of receptor fusion proteins, cells were co-transfected with 0.45  $\mu$ g of Rluc-fused receptor cDNA and 0.45  $\mu$ g of YFP-fused receptor cDNA per 35 mm dish. Two days after transfection, fusion proteins were purified by Wheat Germ Lectin (WGL, Sigma-Aldrich, Saint-Quentin Falavier, France) chromatography as described previously (Blanquart et al., 2005; Boute et al., 2001). After elution with N-acetylglucosamine (0.3 M, Sigma-Aldrich, France), fractions enriched in Rluc activity were pooled, aliquoted and stored at  $-80^\circ$  C for subsequent use.

For the study of conformational changes within the homodimeric or hybrid tyrosine kinase receptor in intact cells, HEK-293 cells were transfected with 0.3  $\mu$ g of Rluc-fused receptor cDNA and either 0.3  $\mu$ g of empty vector or 0.3  $\mu$ g of YFP-fused receptor cDNA per 35 mm dish.

For the study of interaction between receptors and the soluble form of PTP1B, cells were transfected with 0.6  $\mu$ g of IGF1R-Rluc cDNA (wild-type or kinase-dead) or 0.6  $\mu$ g of IRA-Rluc (wild-type or kinase-dead) and either 0.05  $\mu$ g of pEYFP-C1 or 0.3  $\mu$ g of YFP-PTP1B-D181A-Cter cDNA per 35 mm dish. For the measurement of hybrids activation state in intact cells, HEK-293 cells were transfected with 0.6  $\mu$ g of IGF1R<sub>KD</sub>-Rluc cDNA or 0.6  $\mu$ g of IRA<sub>KD</sub>-Rluc cDNA, 0.05  $\mu$ g of pEYFP-C1 or 0.3  $\mu$ g of YFP-PTP1B-D181A-Cter cDNA and either 0.3  $\mu$ g of empty vector, 0.3  $\mu$ g of IRA (untagged) cDNA or 0.3  $\mu$ g of IGF1R (untagged) cDNA per 35 mm dish. One day after transfection, cells were transferred into 96-well microplates (White culturPlate-96, Perkin Elmer, France) at a density of  $3 \times 10^4$  cells per dish. The following day, BRET measurements were performed as described below.



MOL # 26989

### **BRET measurements**

All BRET measurements were performed at room temperature using the Fusion™ microplate analyser (PerkinElmer). BRET measurements on partially purified receptors were performed in a total volume of 50 µl containing 0.02% Triton X100, 4 mM MOPS (pH 7.4), 10 µl (approximately 4 µg of proteins/µl) of concentrated WGL-eluate, and ligands. After 15 minutes of pre-incubation at room temperature, the substrate of luciferase (coelenterazine, Interchim, Montluçon, France) was added to the preparation at a final concentration of 5 µM. Light emission acquisition (at 480 nm and 530 nm) was then started immediately using the Fusion microplate analyser. For the study of conformational changes within the receptors in intact cells, cells were pre-incubated for 15 min in PBS in the presence of 2.5µM coelenterazine. Ligands were then added and light-emission acquisition at 485 and 530 nm was started immediately. For the study of the interaction between receptors and PTP1B, cells were also pre-incubated for 15 min in the presence of 2.5µM coelenterazine. Ligands were then added and the dynamics of the interaction between the receptors and PTP1B was monitored during more than 20 min following ligand addition. BRET measurements were performed every 1.5 - 2 minutes (the interval of time between two measurements for a given well depends on the number of experimental conditions analyzed in the experiment). Each measurement corresponded to the signal emitted by the whole population of cells present in a well. BRET signal was expressed in milliBRET Unit (mBU). The BRET unit has been defined previously as the ratio 530 nm/485 nm obtained when the two partners are present, corrected by the ratio 530 nm/485 nm obtained under the same experimental conditions, when only the partner fused to *Renilla* luciferase is present in the assay (Angers et al., 2000; Boute et al., 2003; Boute et al., 2001).

MOL # 26989

### **Autophosphorylation of receptor fusion proteins in intact cells**

Forty-eight hours after transfection, HEK-293 cells were incubated with different ligands for 5 minutes in DMEM. Proteins were then extracted as described (Boute et al., 2001), subjected to Western-blotting (Issad et al., 1995) and detected using chemiluminescence.

### **Hybrid receptors phosphorylation in intact cells**

HEK-293 cells maintained in DMEM supplemented with 4.5 g/l glucose and 10% fetal bovine serum were seeded at a density of  $2.5 \times 10^5$  cells per 35 mm dish. Transient transfections were performed 1 day later using FuGENE 6 according to the manufacturer's protocol. Cells were transfected with 1  $\mu$ g of IRA<sub>KD</sub>-YFP cDNA or 1 $\mu$ g of IGF1R<sub>KD</sub>-YFP cDNA and either 0.3  $\mu$ g of empty vector, 0.3  $\mu$ g of IRA cDNA or 0.3  $\mu$ g of IGF1R cDNA per 35 mm dish. Forty-eight hours after transfection, HEK-293 cells were incubated with different ligands for 5 minutes in DMEM. Proteins were then extracted as described (Boute et al., 2001), subjected to western-blotting (Issad et al., 1995) and detected using chemiluminescence.

### **Statistical analysis**

Data are expressed as the means  $\pm$  S.E.M. of at least three to six experiments. The statistical comparisons were made using two tailed student's t test for paired values

MOL # 26989

## Results

### Expression of IRA and IGF1R fused to Rluc or YFP in HEK-293 cells

In our previous studies, we have shown that ligand-induced conformational changes within the IRB (Boute et al., 2001) as well as within IGF1R (Blanquart et al., 2005) can be studied by BRET, using receptors fused to either Rluc or YFP. In order to study ligand-induced conformational changes within IRA/IGF1R hybrid receptors, we have also fused the cDNA of IRA to the sequence coding for Rluc and YFP.

Fluorescent microscopy showed that in HEK-293 cells transfected with IRA-YFP alone, IGF1R-YFP alone, or in combination with either IRA-Rluc or IGF1R-Rluc, the fluorescent proteins were detected at the plasma membrane (Fig. 1A). In HEK-293 cells transfected with IRA-YFP, IRA-Rluc or both, 100 nM of insulin or IGF-2 strongly induced the tyrosine-phosphorylation of a protein with an apparent molecular weight of approximately 125-135 kDa, which corresponds to the expected mass of the  $\beta$ -subunit of the IRA protein fused to YFP or Rluc (Fig. 1B, upper panel). At the same concentration (100 nM), IGF-1, which is a poor ligand for IRA, induced a smaller increase in the tyrosine phosphorylation of the chimeric  $\beta$ -subunits. In HEK-293 cells transfected with expression vector for IGF1R-YFP, for IGF1R-Rluc or both, 100 nM of IGF-1 or 100 nM of IGF-2 strongly induced the tyrosine phosphorylation of the chimeric  $\beta$ -subunits (Fig. 1B lower panel). In contrast, at the same concentration (100 nM), insulin, which is a poor ligand for IGF1R, induced a lower increase of the tyrosine phosphorylation of the  $\beta$ -subunits. These results indicate that fusion receptors are correctly expressed at the plasma membrane and are functional for ligand-induced autophosphorylation.

MOL # 26989

## **Ligand-induced conformational changes within IRA/IGF1R hybrid receptors can be detected in intact cells by BRET**

To date, the study of IRA/IGF1R hybrid receptors [ $\alpha\beta$ -IRA/ $\alpha\beta$ -IGF1R] has been largely hampered by the concomitant presence of homodimers of each type ( $[\alpha\beta$ -IRA]<sub>2</sub> and  $[\alpha\beta$ -IGF1R]<sub>2</sub>). We reasoned that BRET represents a unique opportunity to study these hybrid receptors. Indeed, in cells co-transfected with cDNA coding for one type of receptor fused to Rluc and the other type fused to YFP, only heterodimers receptors will be BRET competent (See figure 2).

We first characterized the ligand-induced BRET within IRA and IGF1R homodimeric receptors (Fig. 3). As observed previously for IRB (Boute et al., 2001) and IGF1R (Blanquart et al., 2005), in intact cells, ligand-induced conformational changes result in a modest but reproducible increase in BRET signal in cells transfected with either IRA or IGF1R (Fig. 3A and B). In order to measure ligand-induced conformational changes within IRA/IGF1R hybrid receptors, HEK-293 cells were co-transfected with either IRA-Rluc and IGF1R-YFP cDNA (Fig. 3C) or IGF1R-Rluc and IRA-YFP (Fig. 3D). Ligand-induced conformational changes within hybrid receptors also resulted in a modest but reproducible increase in BRET signal. Therefore, although ligand-induced conformational changes can be detected in hybrid receptors, the magnitude of the effect was rather low in intact cells.

## **Ligand-induced conformational changes within IRA/IGF1R hybrid receptors can be monitored by BRET using partially-purified receptor**

In our previous studies using IRB (Boute et al., 2001) and IGF1R (Blanquart et al., 2005), we observed that ligand-induced BRET (BRET above basal), was much higher *in vitro*, on partially purified receptors, than in intact cells. We therefore purified the different combinations of receptors by chromatography on wheat germ lectin columns (WGL). We observed that the different ligands induced a much stronger increase in BRET signal on

MOL # 26989

partially purified IRA receptors than in intact cells ( $62.5 \pm 1.8$  mBU in presence of insulin,  $56.0 \pm 4.9$  mBU in presence of IGF-1 and to  $61.7 \pm 6.5$  mBU in presence of IGF-2) (Fig. 4A). In addition, as observed in our previous work with IGF-1 receptors (Blanquart et al., 2005), these ligands also induced a much higher increase in BRET signal on partially purified IGF1R receptor than in intact cells ( $38.3 \pm 7.6$  mBU in presence of insulin,  $64.0 \pm 4.0$  mBU in presence of IGF-1 and  $68.6 \pm 7.3$  mBU in presence of IGF-2) (Fig. 4B).

With partially purified hybrid receptors (Fig. 4 C and D), IGF-1 and IGF-2 also induce strong increases in BRET signal ( $67.9 \pm 3.2$  mBU in presence of IGF-1 and  $64.4 \pm 4.4$  mBU in presence of IGF-2 for IRA-Rluc/IGF1R-YFP;  $66.8 \pm 2.0$  mBU in presence of IGF-1 and  $63.9 \pm 3.6$  mBU in presence of IGF-2 for IGF1R-Rluc/IRA-YFP). Insulin-induced BRET signal was much lower ( $25.4 \pm 7.3$  mBU in presence of insulin for IRA-Rluc/IGF1R-YFP;  $24.1 \pm 9.1$  mBU in presence of insulin for IGF1R-Rluc/IRA-YFP) (Fig. 4C and D). Therefore, as observed previously (Boute et al., 2001; Blanquart et al., 2005), partial purification of the fusion receptors improves the ligand-induced BRET. Although the mechanisms responsible for these differences are not understood at the present time, these results suggest that partially purified receptors rather than in intact cells should be used to monitor ligand-induced conformational changes within IRA/IGF1R hybrids by BRET.

### **Monitoring the activation state of IRA/IGF1R hybrid receptors in intact cells.**

The activation state of insulin and IGF-1 receptors is dependent on their autophosphorylation level (Combettes-Souverain and Issad, 1998; Frattali et al., 1992; Kato et al., 1994; De Meyts and Whittaker, 2002). Binding of ligands on these receptors is believed to induce conformational changes that bring the two  $\beta$ -subunits in close proximity, allowing the trans-phosphorylation of one  $\beta$ -subunit by the other (Frattali and Pessin, 1993; Frattali et al., 1992). We reasoned that in cells co-transfected with a cDNA coding for a kinase-dead receptor fused to luciferase and a cDNA coding for a wild-type receptor, trans-phosphorylation of the Rluc-

MOL # 26989

tagged kinase-dead  $\alpha\beta$  moiety by the wild-type  $\alpha\beta$  moiety within heterodimers, should be detectable by BRET by using a YFP-tagged interacting protein which only binds to the tyrosine-phosphorylated  $\beta$ -subunit (Fig. 5).

In previous reports (Blanquart et al., 2005; Boute et al., 2003), we have shown that ligand-induced interaction between IRB or IGF1R and a substrate trapping mutant of PTP1B (PTP1B-D181A) is tightly dependent upon the autophosphorylation of these receptors. Indeed, ligand-induced BRET signal was markedly inhibited by the tyrphostin AG1024, an inhibitor of the tyrosine kinase activity of the IR and IGF1R. Because in the basal state, in the absence of ligand, PTP1B also interacts with the insulin receptor precursor, a high basal BRET signal was also observed in cells transfected with IR-Rluc and YFP-PTP1B-D181A (Boute et al., 2003; Issad et al., 2005). A much lower basal BRET signal was observed with a mutant form of PTP1B, which is not anymore targeted to the endoplasmic reticulum (YFP-PTP1B-D181A-Cter) (Boute et al., 2003). In the present work, we have used this YFP-fused soluble form of PTP1B (YFP-PTP1B-D181A-Cter) as a sensor of the activation state of hybrid receptors. Indeed, this form of PTP1B interacts essentially with ligand-stimulated mature receptors (Boute et al., 2003; Issad et al., 2005).

The cellular localization and expression level of YFP-PTP1B-D181A-Cter in HEK cells were evaluated by fluorescence microscopy (Fig. 6A) and western-blotting (Fig. 6B). As observed previously (Boute et al., 2003), YFP-PTP1B-D181A-Cter was not targeted to the endoplasmic reticulum and had a cellular distribution similar to that of YFP alone. We also characterized the expression and localization of IRA and IGF1R kinase-dead mutants. Fluorescence microscopy (Fig. 6A) showed that, as observed for their wild-type counterparts (Fig. 1A), both mutants were localized at the plasma membrane. In addition, western-blotting experiments (Fig. 6C) indicated that the expression level of these mutants in HEK cells was similar to that of the wild-type receptors.

MOL # 26989

We then characterized the interaction of IRA and IGF1R with the YFP-PTP1B-D181A-Cter protein in intact cells. HEK-293 cells were co-transfected with YFP-PTP1B-D181A-Cter cDNA and either IRA<sub>KD</sub>-Rluc or IRA-Rluc expression vectors (Fig. 7A, B and C). With the IRA<sub>KD</sub>-Rluc, ligands had no effect on BRET signal (Fig. 7A), thereby demonstrating that autophosphorylation of IRA is necessary to observe a ligand-induced increase in BRET. In contrast, with the IRA-Rluc fusion protein, the different ligands induced a rapid and robust increase in this signal (Fig 7B). In cells co-transfected with YFP as a control for YFP-PTP1B-D181A-Cter and either IRA<sub>KD</sub>-Rluc or IRA-Rluc, a very weak basal BRET signal was observed, despite higher expression level of the YFP compared to YFP-PTP1B-D181A-Cter (evaluated by measuring cell fluorescence after exogenous excitation of the YFP, data not shown). Ligands had no effect on this background BRET signal (Fig. 7A and B). Figure 7C shows the means  $\pm$  SEM of ligand-induced BRET signal, measured 20 minutes after addition of 100 nM of each ligand. Insulin and IGF-2 strongly increased the BRET signal ( $93.3 \pm 8.8$  mBU in presence of insulin and  $77.0 \pm 7.8$  in presence of IGF-2). A lower effect was obtained with IGF-1 ( $52.0 \pm 12.1$  mBU in presence of IGF-1).

We also characterized the interaction between IGF1R and PTP1B-Cter in HEK-293 cells co-transfected with YFP-PTP1B-D181A-Cter and either IGF1R<sub>KD</sub>-Rluc or IGF1R-Rluc (Fig. 7D, E and F). With the IGF1R<sub>KD</sub>-Rluc, ligands had no effect on BRET signal (Fig 7D), thereby demonstrating that autophosphorylation of IGF1R is necessary to observe a ligand-induced increase in BRET signal. In contrast, with the IGF1R-Rluc, IGF-1 and IGF-2 induced a rapid and robust increase in this signal, whereas insulin had virtually no effect (Fig 7E). In cells co-transfected with YFP as a control for YFP-PTP1B-D181A-Cter and either IGF1R<sub>KD</sub>-Rluc or IGF1R-Rluc, a very weak basal BRET signal was observed, and ligands had no effects on this signal (Fig. 7D and E). Figure 7F shows the means  $\pm$  SEM of ligand-induced BRET signals, measured 20 minutes after addition of vehicle or 100 nM of each ligand. Whereas IGF-1 and IGF-2 markedly increase the BRET signal ( $34.0 \pm 5.8$  mBU in presence of IGF-1 and  $33 \pm 5.2$

MOL # 26989

in presence of IGF-2), insulin had no significant effect ( $4.6 \pm 1.7$  mBU in presence of insulin). Altogether, these results indicate that the effect of ligands on IRA and IGF1R receptors can be monitored by BRET in intact cells, by using PTP1B-D181A-Cter as a probe for the activation of these receptors.

In order to determine whether this probe can be used to monitor the activation state of IRA/IGF1R hybrid receptors in intact cells, HEK cells were co-transfected with YFP-PTP1B-D181A-Cter, a kinase-dead version of a Rluc-tagged fusion receptor (IRA<sub>KD</sub>-Rluc or IGF1R<sub>KD</sub>-Rluc) and either untagged IRA or IGF1R. Fig. 8A shows results obtained with IRA<sub>KD</sub>-Rluc and YFP-PTP1B-D181A-Cter as BRET partners. Co-transfection with IRA<sub>KD</sub>-Rluc and IRA results in the formation of IRA<sub>KD</sub>-Rluc/IRA heterodimers that permits the detection of ligand-induced BRET signal between IRA<sub>KD</sub>-Rluc and YFP-PTP1B-D181A-Cter (Fig. 8A). Co-transfection with IRA<sub>KD</sub>-Rluc and IGF1R expression vectors results in the formation of IRA<sub>KD</sub>-Rluc/IGF1R hybrid receptors that permits the detection of a ligand-induced BRET between IRA<sub>KD</sub>-Rluc and YFP-PTP1B-D181A-Cter, as shown in figure 8B. In cells co-transfected with YFP as a control for YFP-PTP1B-D181A-Cter, IRA<sub>KD</sub>-Rluc and either untagged IRA or IGF1R, a weak basal BRET signal was obtained and this signal was not increased by the ligands (Fig. 8A and B). Figure 8C shows the means  $\pm$  SEM of basal and ligand-stimulated BRET signal, measured 20 minutes after addition of 100 nM of each ligand. In cells transfected with IRA<sub>KD</sub>-Rluc, YFP-PTP1B-D181A-Cter and IRA, IGF-2 markedly increased BRET signal ( $19.0 \pm 3.5$  mBU in presence of IGF-2). A lower increase was observed with IGF-1 ( $9.6 \pm 3.3$  mBU in presence of IGF-1). In cells co-transfected with IRA<sub>KD</sub>-Rluc, YFP-PTP1B-D181A-Cter and IGF1R, both IGF-1 and IGF-2 induce an increase in BRET signal ( $9.4 \pm 3.1$  mBU in presence of IGF-1 and  $9.6 \pm 2.9$  mBU in presence of IGF-2), indicating that the effect of these ligands on hybrid receptors can be detected by this approach.



MOL # 26989

Fig. 8D, E and F show results obtained with IGF1R<sub>KD</sub>-Rluc and YFP-PTP1B-D181A-Cter as BRET partners. Co-transfection with either IGF1R<sub>KD</sub>-Rluc and IGF1R results in the formation of IGF1R<sub>KD</sub>-Rluc/IGF1R hybrids that permits the detection of ligand-induced BRET signal between IGF1R<sub>KD</sub>-Rluc and YFP-PTP1B-D181A-Cter (Fig. 8D). Similarly, co-transfection with IGF1R<sub>KD</sub>-Rluc and IRA results in the formation of IGF1R<sub>KD</sub>-Rluc/IRA hybrids that permits the detection of ligand-induced BRET signal between IGF1R<sub>KD</sub>-Rluc and YFP-PTP1B-D181A-Cter (Figure 8E). In cells co-transfected with YFP as a control for YFP-PTP1B-D181A-Cter, IGF1R<sub>KD</sub>-Rluc and either untagged IRA or IGF1R, a weak basal BRET signal was obtained, and this signal was not increased by the ligands (Fig. 8D and E). Figure 8F shows the means  $\pm$  SEM of ligand-induced BRET signals, measured 20 minutes after addition of 100 nM of each ligand. In cells transfected with YFP-PTP1B-D181A-Cter, IGF1R<sub>KD</sub>-Rluc and IGF1R, both IGF-1 and IGF-2 increased the BRET signal ( $10.8 \pm 1.0$  mBU in presence of IGF-1 and  $9.2 \pm 0.4$  mBU in presence of IGF-2). In cells co-transfected with IGF1R<sub>KD</sub>-Rluc, YFP-PTP1B-D181A-Cter and IRA, both IGF-1 and IGF-2 increased BRET signal ( $18.0 \pm 2.6$  mBU in presence of IGF-1 and  $18.5 \pm 3.1$  mBU in presence of IGF-2). Altogether, our results indicate that the effects of ligands on IRA/IGF1R hybrid receptors can be detected in cells expressing IRA<sub>KD</sub>-Rluc/IGF1R (Fig. 8C) or IGF1R<sub>KD</sub>-Rluc/IRA (Fig. 8F). To determine whether these BRET signals indeed reflect trans-phosphorylation of the kinase-dead  $\alpha\beta$  moiety by the wild-type  $\alpha\beta$  moiety, HEK-293 cells were transfected with a YFP-fused kinase-dead receptor and a non-tagged wild-type receptor. Taking advantage of the higher molecular weight of the YFP-tagged fusion protein, the trans-phosphorylation of the YFP-fused kinase-dead receptor was evaluated by western-blot using anti-phosphotyrosine antibody (4G10). As expected, in cells transfected with the IRA<sub>KD</sub>-YFP cDNA, no phosphorylation of the chimeric protein could be detected (Fig. 9A). Co-transfection of cells with IRA<sub>KD</sub>-YFP and IRA is expected to result in the expression of IRA/IRA receptors and IRA<sub>KD</sub>-YFP/IRA receptors. IGF-2, and to a lower extent IGF-1, induced a marked trans-

MOL # 26989

phosphorylation of IRA<sub>KD</sub>-YFP by IRA ( $5.0 \pm 0.6$  fold in presence of IGF-2 and  $3.7 \pm 0.5$  fold in presence of IGF-1) (Fig. 9A and B). Co-transfection of HEK-293 cells with IRA<sub>KD</sub>-YFP and IGF1R is expected to result in the formation of IGF1R/IGF1R homodimer receptors and IRA<sub>KD</sub>-YFP/IGF1R hybrid receptors. IGF-1 and IGF-2 induced a modest but detectable trans-phosphorylation of IRA<sub>KD</sub>-YFP by IGF1R ( $3.0 \pm 0.5$  fold in presence of IGF-1 and  $2.5 \pm 0.4$  fold in presence of IGF-2) (Fig. 9A and B).

The converse experiment was also performed (Fig. 9C and D). In cells transfected with IGF1R<sub>KD</sub>-YFP alone, no phosphorylation of the chimeric protein could be detected (Fig. 9C). Co-transfection of cells with IGF1R<sub>KD</sub>-YFP and IGF1R is expected to result in the formation of IGF1R/IGF1R receptors and IGF1R<sub>KD</sub>-YFP/IGF1R receptors. Trans-phosphorylation of the IGF1R<sub>KD</sub>-YFP by the IGF1R could be detected after stimulation with IGF-1 ( $3.8 \pm 0.7$  fold) and IGF-2 ( $3.2 \pm 0.6$  fold) (Fig. 9C and D). Co-transfection of HEK-293 cells with IGF1R<sub>KD</sub>-YFP and IRA is expected to result in the formation of IRA/IRA homodimers and IGF1R<sub>KD</sub>-YFP/IRA hybrids. Trans-phosphorylation of IGF1R<sub>KD</sub>-YFP by IRA could be detected after stimulation with IGF-1 ( $4.2 \pm 0.5$  fold) and IGF-2 ( $4.2 \pm 0.4$  fold) (Fig. 9C and D).

In both configurations, the trans-phosphorylation of YFP-fused kinase-dead correlated with ligand-induced BRET signal between YFP-PTP1B-D181A-Cter and the Rluc-fused kinase-dead receptor (Fig. 8). Therefore, this demonstrates that the activation of IRA/IGF1R hybrid receptors can be monitored in real time, in living cells by using the BRET technology.

MOL # 26989

## Discussion

IRA/IGF1 hybrid receptors have been involved in a number of tumors (Belfiore et al., 1999; Pandini et al., 1999). Thus, the discovery of molecules capable of inhibiting the activities of these receptors may be important for cancer therapy. However, cells expressing hybrid receptors also express homoreceptors of each type, precluding the specific study of heterodimers. In this work, we aimed to develop procedures, based on BRET, to monitor specifically the activity of these hybrid receptors. The first approach was based on the idea that, in cells co-transfected with the cDNA coding for one type of receptor fused to Rluc and the other type to YFP, only hybrid heterodimer receptors will contain one  $\beta$ -subunit fused to luciferase and the other  $\beta$ -subunit fused to YFP. Therefore, in these cells, only hybrid receptors will be BRET competent. We observed that this simple principle indeed allows to monitor ligand-induced conformational changes *in vitro*, using receptors partially purified from cells co-transfected with IRA and IGF1R tagged with either Rluc or YFP. In living cells, ligand-induced conformational changes within hybrid receptors resulted in much smaller increases in BRET signal. This is a reminiscence of our previous results with IRB (Boute et al., 2001) and IGF1R (Blanquart et al., 2005) and confirms the notion that the use of partially purified receptor is more suitable for monitoring conformational changes within these receptors by BRET. Although studies on purified IR/IGF1R hybrid receptors have already been performed, they generally involved multi-steps protocols, including sequential immunoprecipitation using antibodies to specifically deplete IR and IGF1R homodimers from the WGL eluates (Moss and Livingston, 1993; Soos et al., 1993; Soos and Siddle, 1989). These time-consuming procedures may, in addition, affect the results according to the relative efficiency and selectivity of the antibodies used during the immuno-depletion steps. In contrast, our BRET method is a single-step procedure that allows the direct study of IR/IGF1R heterodimeric receptors in WGL eluates, without having to separate them from IR and IGF1R homodimers. Therefore, our procedure is much simpler and faster and could be of

MOL # 26989

considerable interest in high-throughput screening assays for the search of molecules that specifically regulate IR/IGF1R hybrids.

Although the use of an *in vitro* assay presents a number of advantages for the search of molecules capable of modulating the activity of receptors (Blanquart et al., 2005; Boute et al., 2002; Issad et al., 2002), it also presents a number of limitations. Molecules that are not cell-permeable may act on purified receptors but not on intact cells. Conversely, some molecules may need a cellular environment (plasma membrane insertion of the receptor, preservation of interaction of the receptor with cytosolic partners) to exert their effects. Thus, the activity of such molecules will only be detected in an intact cell assay. The development of an *in vivo* assay, that permits to study specifically IRA/IGF1R hybrids, appears therefore necessary. Using co-transfection of Rluc-tagged kinase-dead mutants, in association with their wild-type untagged counterparts, and a YFP-tagged soluble form of PTP1B, known to bind to the activated tyrosine-phosphorylated receptor, we have shown that the activation state of hybrid receptors can be specifically measured, in real time, in intact living cells. The validity of the method was confirmed by the good correlation of results obtained by BRET with those obtained by biochemical methods based on a similar principle (co-transfection of a YFP-tagged kinase dead receptor mutant and its wild-type untagged counterpart). In these experiments, detection of phosphorylation of the mutant receptor was rendered possible by its higher molecular weight, as a result of its fusion with YFP. In BRET experiments, the recovery of ligand-induced BRET signal between Rluc-tagged kinase-dead receptor and YFP-PTP1B-D181A-Cter tended to be better with the IGF1R<sub>KD</sub>-Rluc/IRA hybrids than with IRA<sub>KD</sub>-Rluc/IGF1R hybrids (compare panels F and C in Fig. 8). In line with this result, phosphorylation of IGF1R<sub>KD</sub>-YFP by IRA was more readily detected than phosphorylation of IRA<sub>KD</sub>-YFP by IGF1R (compare panels A and C in Fig. 9). This suggests that IGF1R<sub>KD</sub>-Rluc/IRA hybrid rather than IRA<sub>KD</sub>-Rluc/IGF1R should be used in a BRET assay with YFP-PTP1B-D181A-Cter in intact cells.

MOL # 26989

In summary, we have developed tools based on the BRET technology to study the activation state of IRA/IGF1R hybrids, both *in vitro* and in intact cells. We have shown that ligand-induced conformational changes within hybrids can easily be measured by BRET using partially purified receptors. In addition, we have shown that the effect of ligands on IRA/IGF1R hybrids receptors can also be monitored by BRET, in real time, in intact living cells. These assays may be used for the search of molecules of therapeutic interest for the treatment of cancers in which IRA/IGF1R hybrids have been involved. In addition, this work constitute a proof of principle for the development of BRET assays specifically designed to monitor the activity of other tyrosine-kinase hybrid receptors, by using Rluc-tagged kinase-dead receptors and YFP-tagged interacting partners. Indeed, heterodimerization within members of the same family have been described for other tyrosine kinase receptors, such as those of the EGFR family, and heterodimerisation of these receptors also appears to play crucial roles in their oncogenic potential (Olayioye et al., 2000; Yarden and Sliwkowski, 2001).

MOL # 26989

### **Acknowledgements**

pECE-IRA was kindly provided by Dr. Ozan, Institut Cochin, Paris, France. We thank Christian Fédérici for useful advises on statistical analysis.

MOL # 26989

## References

- Angers S, Salahpour A, Joly E, Hilaiet S, Chelsky D, Dennis M and Bouvier M (2000) Detection of beta 2-adrenergic receptor dimerization in living cells using bioluminescence resonance energy transfer (BRET). *Proc Natl Acad Sci U S A* **97**:3684-3689.
- Belfiore A, Pandini G, Vella V, Squatrito S and Vigneri R (1999) Insulin/IGF-I hybrid receptors play a major role in IGF-I signaling in thyroid cancer. *Biochimie* **81**:403-407.
- Blanquart C, Boute N, Lacasa D and Issad T (2005) Monitoring the activation state of the insulin-like growth factor-1 receptor and its interaction with protein tyrosine phosphatase 1B using bioluminescence resonance energy transfer. *Mol Pharmacol* **68**:885-894.
- Boute N, Boubekeur S, Lacasa D and Issad T (2003) Dynamics of the interaction between the insulin receptor and protein tyrosine-phosphatase 1B in living cells. *EMBO Rep* **4**:313-319.
- Boute N, Jockers R and Issad T (2002) The use of resonance energy transfer in high-throughput screening: BRET versus FRET. *Trends Pharmacol Sci* **23**:351.
- Boute N, Pernet K and Issad T (2001) Monitoring the activation state of the insulin receptor using bioluminescence resonance energy transfer. *Mol Pharmacol* **60**:640-645.
- Combettes-Souverain M and Issad T (1998) Molecular basis of insulin action. *Diabetes Metab* **24**:477-489.
- De Meyts P and Whittaker J (2002) Structural biology of insulin and IGF1 receptors: implications for drug design. *Nat Rev Drug Discov* **1**:769-783.
- Denley A, Wallace JC, Cosgrove LJ and Forbes BE (2003) The insulin receptor isoform exon 11- (IR-A) in cancer and other diseases: a review. *Horm Metab Res* **35**:778-785.

MOL # 26989

Ellis L, Clauser E, Morgan DO, Edery M, Roth RA and Rutter WJ (1986) Replacement of insulin receptor tyrosine residues 1162 and 1163 compromises insulin-stimulated kinase activity and uptake of 2-deoxyglucose. *Cell* **45**:721-732.

Frasca F, Pandini G, Scalia P, Sciacca L, Mineo R, Costantino A, Goldfine ID, Belfiore A and Vigneri R (1999) Insulin receptor isoform A, a newly recognized, high-affinity insulin-like growth factor II receptor in fetal and cancer cells. *Mol Cell Biol* **19**:3278-3288.

Frattali AL and Pessin JE (1993) Relationship between alpha subunit ligand occupancy and beta subunit autophosphorylation in insulin/insulin-like growth factor-1 hybrid receptors. *J Biol Chem* **268**:7393-7400.

Frattali AL, Treadway JL and Pessin JE (1992) Transmembrane signaling by the human insulin receptor kinase. Relationship between intramolecular beta subunit trans- and cis-autophosphorylation and substrate kinase activation. *J Biol Chem* **267**:19521-19528.

Issad T, Boute N, Boubekeur S and Lacasa D (2005) Interaction of PTPB with the insulin receptor precursor during its biosynthesis in the endoplasmic reticulum. *Biochimie* **87**:111-116.

Issad T, Boute N and Pernet K (2002) A homogenous assay to monitor the activity of the insulin receptor using Bioluminescence Resonance Energy Transfer. *Biochem Pharmacol* **64**:813-817.

Issad T, Combettes M and Ferre P (1995) Isoproterenol inhibits insulin-stimulated tyrosine phosphorylation of the insulin receptor without increasing its serine/threonine phosphorylation. *Eur J Biochem* **234**:108-115.

Kato H, Faria TN, Stannard B, Roberts CT, Jr. and LeRoith D (1994) Essential role of tyrosine residues 1131, 1135, and 1136 of the insulin-like growth factor-I (IGF-I) receptor in IGF-I action. *Mol Endocrinol* **8**:40-50.



MOL # 26989

Lacasa D, Boute N and Issad T (2005) Interaction of the insulin receptor with the receptor-like protein tyrosine phosphatases PTPalpha and PTPepsilon in living cells. *Mol Pharmacol* **67**:1206-1213.

Moller DE, Yokota A, Caro JF and Flier JS (1989) Tissue-specific expression of two alternatively spliced insulin receptor mRNAs in man. *Mol Endocrinol* **3**:1263-1269.

Moss AM and Livingston JN (1993) Distinct beta-subunits are present in hybrid insulin-like-growth-factor-1 receptors in the central nervous system. *Biochem J* **294** ( Pt 3):685-692.

Mosthaf L, Grako K, Dull TJ, Coussens L, Ullrich A and McClain DA (1990) Functionally distinct insulin receptors generated by tissue-specific alternative splicing. *Embo J* **9**:2409-2413.

Nouaille S, Blanquart C, Zilberfarb V, Boute N, Perdereau D, Roix J, Burnol AF and Issad T (2006) Interaction with Grb14 results in site-specific regulation of tyrosine phosphorylation of the insulin receptor. *EMBO Rep* **7**:512-518.

O'Connor R (2003) Regulation of IGF-I receptor signaling in tumor cells. *Horm Metab Res* **35**:771-777.

Olayioye MA, Neve RM, Lane HA and Hynes NE (2000) The ErbB signaling network: receptor heterodimerization in development and cancer. *Embo J* **19**:3159-3167.

Pandini G, Frasca F, Mineo R, Sciacca L, Vigneri R and Belfiore A (2002) Insulin/insulin-like growth factor I hybrid receptors have different biological characteristics depending on the insulin receptor isoform involved. *J Biol Chem* **277**:39684-39695.

Pandini G, Vigneri R, Costantino A, Frasca F, Ippolito A, Fujita-Yamaguchi Y, Siddle K, Goldfine ID and Belfiore A (1999) Insulin and insulin-like growth factor-I (IGF-I) receptor overexpression in breast cancers leads to insulin/IGF-I hybrid receptor overexpression: evidence for a second mechanism of IGF-I signaling. *Clin Cancer Res* **5**:1935-1944.

MOL # 26989

- Pollak MN (2004) Insulin-like growth factors and neoplasia. *Novartis Found Symp* **262**:84-98; discussion 98-107, 265-108.
- Sciacca L, Costantino A, Pandini G, Mineo R, Frasca F, Scalia P, Sbraccia P, Goldfine ID, Vigneri R and Belfiore A (1999) Insulin receptor activation by IGF-II in breast cancers: evidence for a new autocrine/paracrine mechanism. *Oncogene* **18**:2471-2479.
- Soos MA, Field CE and Siddle K (1993) Purified hybrid insulin/insulin-like growth factor-I receptors bind insulin-like growth factor-I, but not insulin, with high affinity. *Biochem J* **290 ( Pt 2)**:419-426.
- Soos MA and Siddle K (1989) Immunological relationships between receptors for insulin and insulin-like growth factor I. Evidence for structural heterogeneity of insulin-like growth factor I receptors involving hybrids with insulin receptors. *Biochem J* **263**:553-563.
- Soos MA, Whittaker J, Lammers R, Ullrich A and Siddle K (1990) Receptors for insulin and insulin-like growth factor-I can form hybrid dimers. Characterisation of hybrid receptors in transfected cells. *Biochem J* **270**:383-390.
- Vella V, Pandini G, Sciacca L, Mineo R, Vigneri R, Pezzino V and Belfiore A (2002) A novel autocrine loop involving IGF-II and the insulin receptor isoform-A stimulates growth of thyroid cancer. *J Clin Endocrinol Metab* **87**:245-254.
- Vella V, Sciacca L, Pandini G, Mineo R, Squatrito S, Vigneri R and Belfiore A (2001) The IGF system in thyroid cancer: new concepts. *Mol Pathol* **54**:121-124.
- Xu Y, Piston DW and Johnson CH (1999) A bioluminescence resonance energy transfer (BRET) system: application to interacting circadian clock proteins. *Proc Natl Acad Sci U S A* **96**:151-156.
- Yarden Y and Sliwkowski MX (2001) Untangling the ErbB signalling network. *Nat Rev Mol Cell Biol* **2**:127-137.

MOL # 26989

**Footnotes.**

This work was supported by the Association pour la Recherche sur le Cancer (Grant n° 3781) and by the Ligue contre le Cancer, Comité de Paris (Grant n° R04/75/75). C.G-Y hold a grant from the Fondation pour la Recherche Médicale.

Address for reprint requests:

Dr. Tarik ISSAD,

Institut Cochin, Department of Cell Biology,

22 Rue Méchain, 75014 PARIS, FRANCE

Tel: (331)-40-51-64-09

Fax: (331)-40-51-64-30

email: [issad@cochin.inserm.fr](mailto:issad@cochin.inserm.fr)

MOL # 26989

## Legends for figures:

**Figure 1:** Functional expression of chimeric insulin and IGF-1 receptors.

(A) HEK-293 cells were transfected with YFP alone or different combinations of Rluc or YFP-tagged IRA, IGF1R or both. Localisation of the proteins was observed using fluorescent microscopy. (B) HEK-293 cells transfected with either empty vector (Mock), IRA-YFP, IRA-Rluc, IGF1R-YFP, IGF1R-Rluc, IRA-YFP + IRA-Rluc, or IGF1R-YFP + IGF1R-Rluc. 48 h after transfection, cells were incubated for 5 minutes in the absence or presence of 100 nM IGF-1, 100 nM IGF-2 or 100 nM insulin. Proteins were extracted and autophosphorylation on tyrosine residues was evaluated by immunoblotting using an anti-phosphotyrosine antibody (4G10). The amount of IRA and IGF1R loaded in each lane was evaluated by immunoblotting with an anti-IR $\beta$  or an anti-IGF1R $\beta$  antibody, respectively.

**Figure 2:** Principle of a BRET assay to specifically monitor IRA/IGF1R hybrids

Co-transfection of HEK-293 cells with IGF1R-Rluc and IRA-YFP result in the formation of IGF1R-Rluc/IGF1R-Rluc and IRA-YFP/IRA-YFP homodimeric receptors and IGF1R-Rluc/IRA-YFP hybrid receptors. Only IGF1R-Rluc/IRA-YFP hybrid receptors can produce a BRET signal, allowing direct monitoring of hybrid receptors.

**Figure 3:** Effect of ligands on BRET signal in intact cells.

HEK-293 cells were co-transfected with either IRA-Rluc and IRA-YFP (A), IGF1R-Rluc and IGF1R-YFP (B), IRA-Rluc and IGF1R-YFP (C) or IGF1R-Rluc and IRA-YFP (D). BRET signal was measured on intact cells in absence or presence of 100 nM of IGF-1, IGF-2 or insulin as described under *Materials and Methods*. Results are the means  $\pm$  S.E.M. of six independent experiments. NS,  $P > 0.05$ , \*,  $P < 0.05$ , \*\*,  $P < 0.005$ , \*\*\*,  $P < 0.001$ .

MOL # 26989

**Figure 4:** Effect of ligands on BRET signal *in vitro* using partially purified receptors.

HEK-293 cells were co-transfected with either IRA-Rluc and IRA-YFP (A), IGF1R-Rluc and IGF1R-YFP (B), IRA-Rluc and IGF1R-YFP (C) or IGF1R-Rluc and IRA-YFP (D). Fusion receptors were partially purified by WGL chromatography. BRET assays were performed *in vitro* in the absence or in presence of 100 nM of IGF-1, IGF-2 or insulin as described under *Materials and Methods*. Results are the means  $\pm$  S.E.M. of four independent experiments. \*,  $P < 0.05$ , \*\*,  $P < 0.01$ , \*\*\*,  $P < 0.001$ .

**Figure 5:** Principle of a BRET-based assay to monitor, in real time, the activation state of IRA/IGF1R hybrid receptors in intact cells.

In HEK-293 cells co-transfected with YFP-PTP1B-D181A-Cter, IGF1R<sub>KD</sub>-Rluc and IRA result in the formation of IRA/IRA and IGF1R<sub>KD</sub>-Rluc/IGF1R<sub>KD</sub>-Rluc homodimeric receptors, and IGF1R<sub>KD</sub>-Rluc/IRA hybrid receptors. IRA/IRA receptors can autophosphorylate and interact with YFP-PTP1B-D181A-Cter but cannot produce BRET signal, because they do not have Rluc activity. IGF1R<sub>KD</sub>-Rluc/IGF1R<sub>KD</sub>-Rluc cannot autophosphorylate. Therefore, they cannot recruit YFP-PTP1B-D181A-Cter upon ligand stimulation and cannot contribute to ligand-induced BRET signal. In IGF1R<sub>KD</sub>-Rluc /IRA hybrid receptors, IRA  $\beta$ -subunit can trans-phosphorylate the IGF1R<sub>KD</sub>-Rluc  $\beta$ -subunit in presence of ligands. The tyrosine-phosphorylated IGF1R<sub>KD</sub>-Rluc  $\beta$ -subunit will then recruit YFP-PTP1B-D181A-Cter, resulting in the production of a ligand-induced BRET signal. Therefore, in this system, only hybrid receptors can produce a ligand-induced BRET signal.

**Figure 6:** Expression and localization of the YFP-PTP1B-D181A-Cter and kinase dead receptor fusion proteins.

(A) HEK-293 cells were transfected with YFP alone, YFP-PTP1B-D181A-Cter, IRA<sub>KD</sub>-YFP or IGF1R<sub>KD</sub>-YFP. Localization of the proteins was observed by fluorescent microscopy. (B)

MOL # 26989

HEK-293 cells were transfected with empty vector or YFP-PTP1B-D181A-Cter (0.3 $\mu$ g/well). 48 h after transfection, proteins were extracted and PTP1B was revealed by immunoblotting with an anti-PTP1B antibody. (C) HEK-293 cells were transfected with either IRA-Rluc, IRA<sub>KD</sub>-Rluc, IGF1R-RLuc or IGF1R<sub>KD</sub>-Rluc (0.6 $\mu$ g/well). 48 h after transfection, proteins were extracted and the expression level of wild-type and kinase-dead mutants of IRA and IGF1R was evaluated by immunoblotting with an anti-IR $\beta$  or an anti-IGF1R $\beta$  antibody, respectively.

**Figure 7:** Characterization of the interaction of IRA and IGF1R homodimers with YFP-PTP1B-D181A-Cter in intact living cells.

HEK-293 cells were co transfected with YFP-PTP1B-D181A-Cter or YFP and either wild-type or kinase-dead version of IRA-Rluc or IGF1R-Rluc. BRET was measured in real time, in intact living cells, in the absence or presence of 100 nM of IGF-1, IGF-2 or insulin.

(A, B) Representative experiments showing the dynamics of interaction of IRA<sub>KD</sub>-Rluc or IRA-Rluc with YFP-PTP1B-D181A-Cter or YFP. (C) Graphic representation of ligand-induced BRET (BRET above basal) measured 20 minutes after addition of 100 nM of IGF-1, IGF-2 or insulin (results are the means  $\pm$  S.E.M. of three independent experiments. \*,  $P < 0.05$ , \*\*  $P < 0.01$ ). (D, E) Representative experiments showing the dynamics of interaction of IGF1R<sub>KD</sub>-Rluc or IGF1<sub>KD</sub>-Rluc with YFP-PTP1B-D181A-Cter or YFP. (F) Graphic representation of ligand-induced BRET (BRET above basal) measured 20 minutes after addition of 100 nM of IGF-1, IGF-2 or insulin (results are the means  $\pm$  S.E.M. of three independent experiments. \*,  $P < 0.05$ ).

MOL # 26989

**Figure 8:** Monitoring in real time the effects of ligands on IRA/IGF1R hybrid receptors in intact cells by BRET.

(A, B) HEK-293 cells were transfected with IRA<sub>KD</sub>-Rluc, YFP-PTP1B-D181A-Cter or YFP and either IRA (A) or IGF1R (B). BRET was measured in real time, in intact living cells, in the absence or presence of 100 nM of IGF-1 or IGF-2. Representative experiments are shown. (C) Graphic representation of ligand-induced BRET signal (BRET above basal) measured 20 minutes after addition of 100 nM of IGF-1 or IGF-2 (results are the means  $\pm$  S.E.M. of five independent experiments. \*,  $P < 0.05$ , \*\*,  $P < 0.01$ ). (D, E) HEK-293 cells were transfected with IGF1R<sub>KD</sub>-Rluc, YFP-PTP1B-D181A-Cter or YFP and either IGF1R (D) or IRA (E). BRET was measured in real time, in intact living cells, in the absence or presence of 100 nM of IGF-1 or IGF-2. Representative experiments are shown. (F), Graphic representation of ligand induced-BRET signals (BRET above basal) measured 20 minutes after addition of 100 nM of IGF-1 or IGF-2 (results are the means  $\pm$  S.E.M. of four independent experiments. \*\*,  $P < 0.01$ , \*\*\*,  $P < 0.001$ ).

**Figure 9:** IRA/IGF1R hybrid receptors trans-phosphorylation.

(A), HEK-293 cells were transfected with IRA<sub>KD</sub>-YFP and either pcDNA3 empty vector, IRA or IGF1R. 48 h after transfection, cells were incubated for 5 minutes in the absence or presence of 100 nM of IGF-1 or IGF-2. Proteins were extracted and phosphorylation on tyrosine residues was evaluated by immunoblotting using an anti-phosphotyrosine antibody (4G10). The amount of IRA<sub>KD</sub>-YFP, IRA and IGF1R loaded in each lane was evaluated by immunoblotting with an anti-IR $\beta$  or an anti-IGF1R $\beta$  antibody, respectively. (B) Densitometric analysis of the anti-phosphotyrosine signal corrected by the IRA<sub>KD</sub>-YFP signal (results are the means  $\pm$  S.E.M. of four independent experiments. \*,  $P < 0.05$ ; \*\*,  $P < 0.01$ ). (C) HEK-293 cells were co-transfected with IGF1R<sub>KD</sub>-YFP and either pcDNA3 empty vector, IRA or IGF1R. 48 h after transfection, cells were incubated for 5 minutes in the absence or

MOL # 26989

presence of 100 nM of IGF-1 or IGF-2. Proteins were extracted and phosphorylation on tyrosine residues was evaluated by immunoblotting using an anti-phosphotyrosine antibody (4G10). The amount of IGF1R<sub>KD</sub>-YFP, IGF1R and IRA loaded in each lane was evaluated by immunoblotting with an anti-IGF1R $\beta$  or an anti-IR $\beta$  antibody, respectively. (D) Densitometric analysis of the anti-phosphotyrosine signal corrected by the IRA<sub>KD</sub>-YFP signal (results are the means  $\pm$  S.E.M. of four independent experiments. \*,  $P < 0.05$ ).



Figure 1

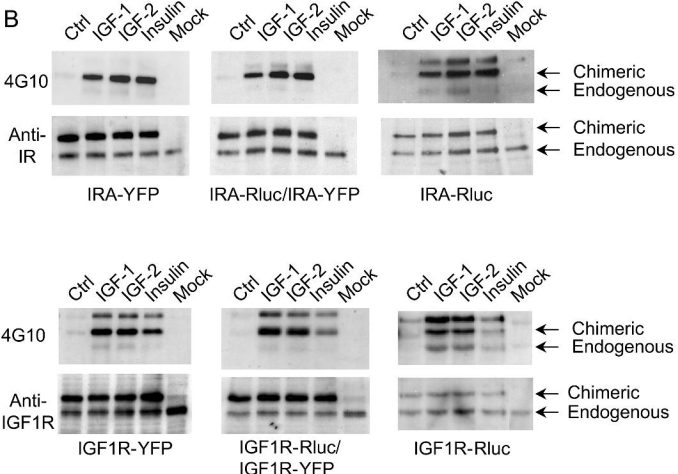
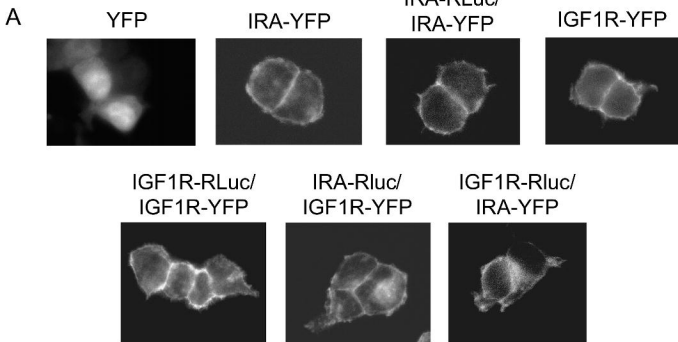


Figure 2

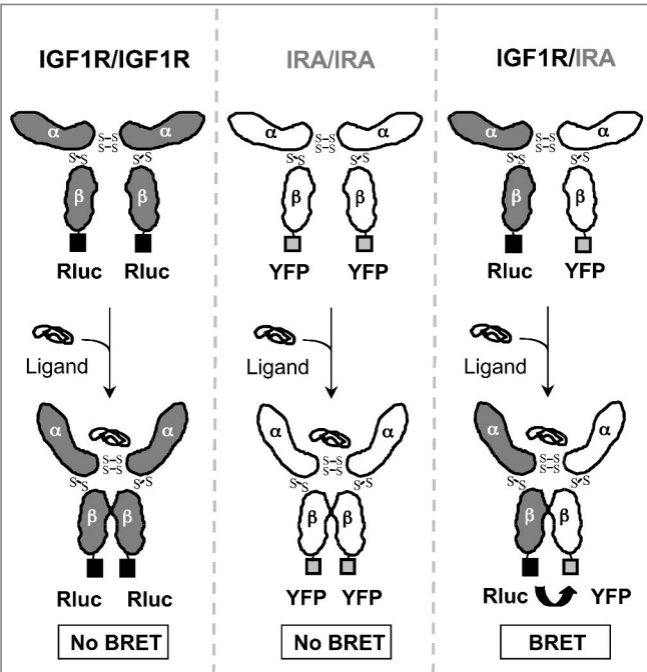


Figure 3

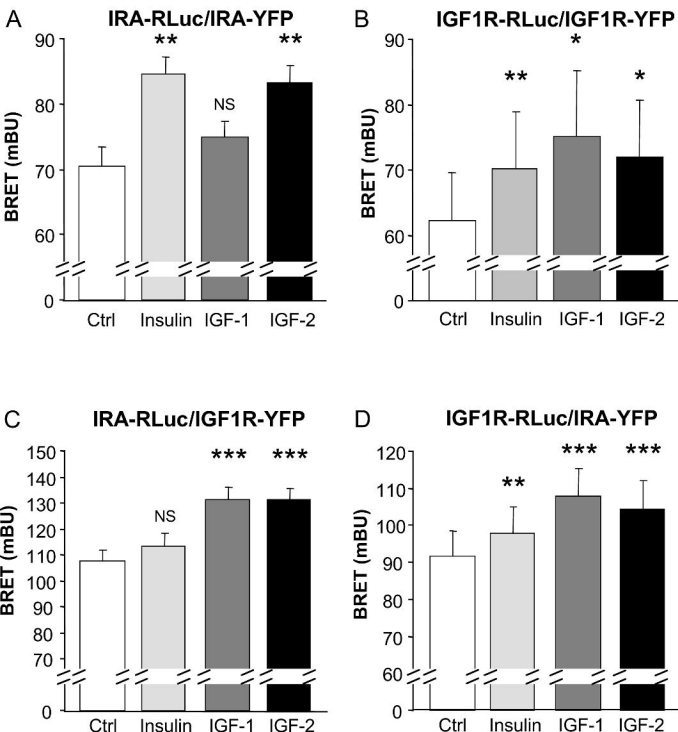


Figure 4

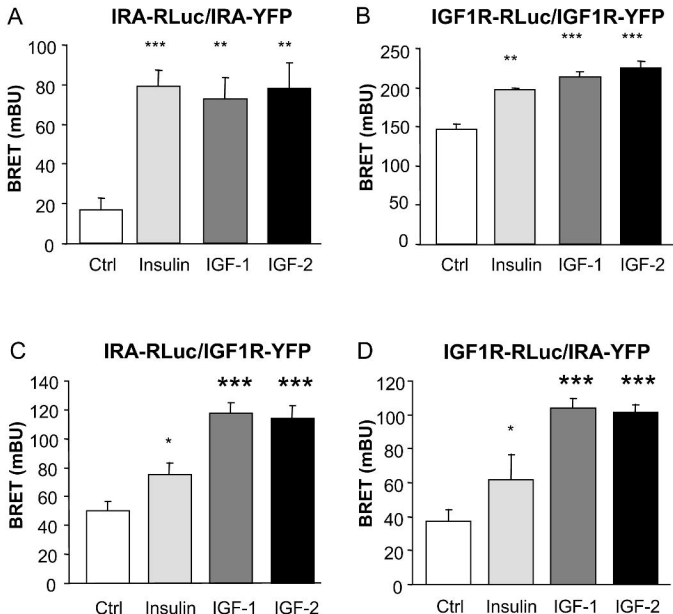


Figure 5

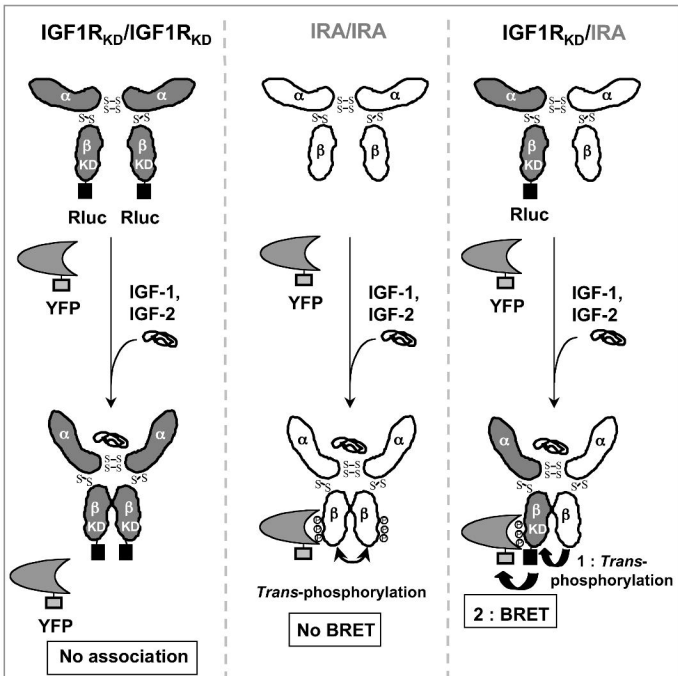
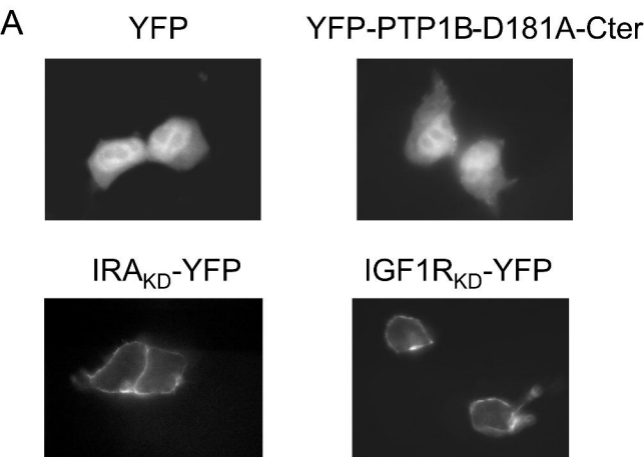
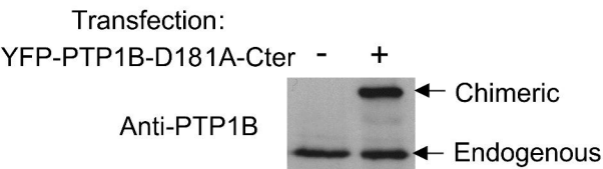


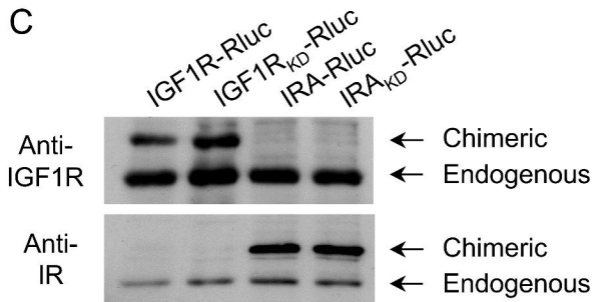
Figure 6

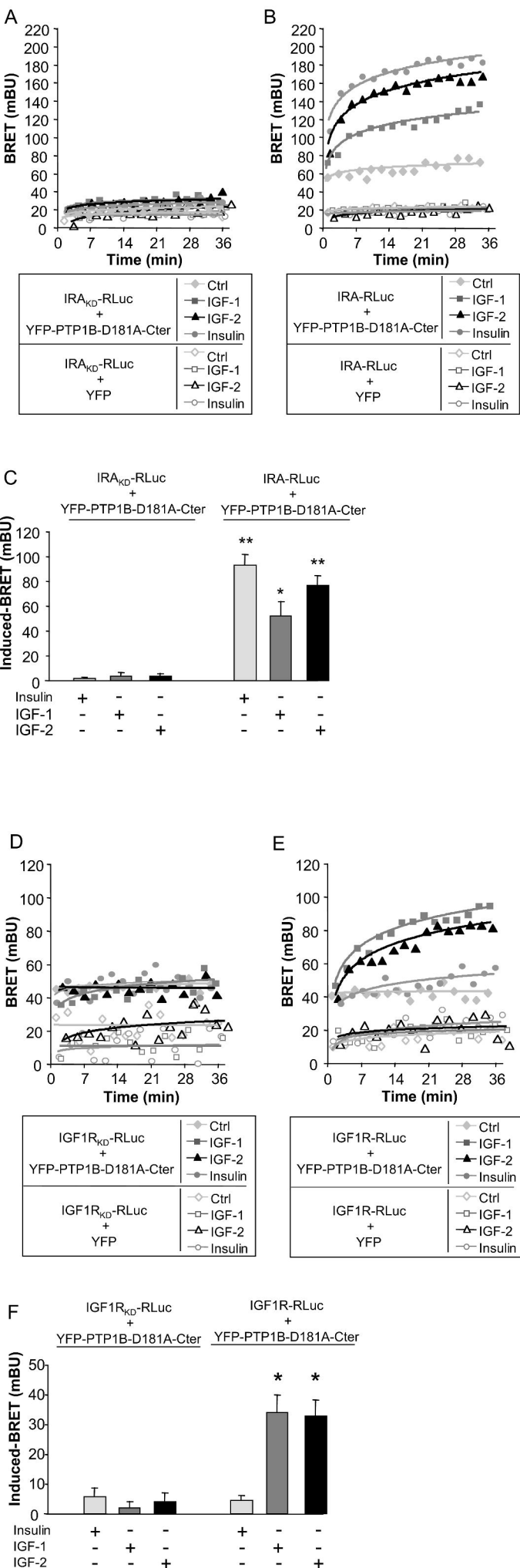


**B**



**C**





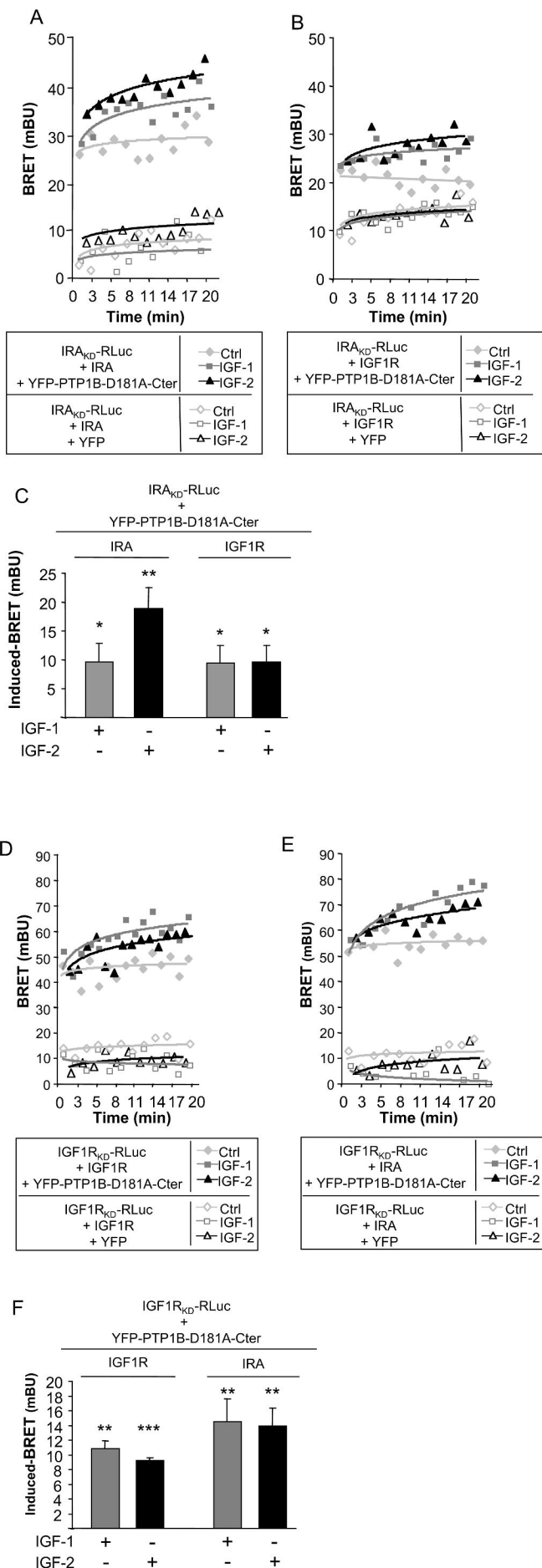




Figure 9

